

Synthesis and Characterization of Novel Oxo-Bridged Dinuclear and Hydroxo-Bridged Trinuclear Chromium(III) Assemblies

Anthony Harton,¹ Katisha Terrell,¹ John C. Huffman,² Chris MacDonald,² Alicia Beatty,³ Sichu Li,⁴ Charles J. O'Connor,^{*4} and John B. Vincent^{*1}

Department of Chemistry, University of Alabama, Tuscaloosa, Alabama 35487-0336, Molecular Structure Center, Indiana University, Bloomington, Indiana 47405, Department of Chemistry, Washington University, St. Louis, Missouri 63130, and Department of Chemistry, University of New Orleans, New Orleans, Louisiana 70148

Received October 15, 1996[⊗]

The structural and spectroscopic properties of a novel dinuclear chromium–oxo and a trinuclear chromium–hydroxo complex are reported. The dinuclear assembly, $[\text{Cr}_2(\mu\text{-O})_2(\mu\text{-O}_2\text{CMe})(\text{bpy})_2(\text{H}_2\text{O})_2]\text{ClO}_4 \cdot \text{bpy} \cdot [\text{bpyH}]\text{-ClO}_4$ (**1**), crystallizes in the monoclinic space group Cc with $a = 16.8259(8)$ Å, $b = 21.9622(11)$ Å, $c = 14.6056(8)$ Å, $\beta = 122.1830(10)^\circ$, $V = 4568.0(4)$ Å³, and $Z = 4$. The structure was refined with 4378 observed reflections having $F > 2.0\sigma(F)$, giving final R factors of 0.0721 and 0.1305 for R and R_{w2} , respectively. The $[\text{Cr}_2(\mu\text{-O})_2(\mu\text{-O}_2\text{CMe})]^+$ core is structurally akin to those of recently reported isoelectronic $[\text{Mn}_2(\mu\text{-O})_2(\mu\text{-O}_2\text{CMe})]^{3+}$ complexes. The trinuclear assembly, $[\text{Cr}_3(\mu\text{-OH})_2(\mu\text{-O}_2\text{CMe})_4(\text{O}_2\text{CMe})_2(\text{bpy})_2]\text{ClO}_4 \cdot 5\text{CHCl}_3$ (**2**), crystallizes in the triclinic space group $P\bar{1}$ with $a = 16.104(5)$ Å, $b = 17.623(5)$ Å, $c = 12.236(3)$ Å, $\alpha = 93.33(1)^\circ$, $\beta = 92.81(1)^\circ$, $\gamma = 64.84(1)^\circ$, $V = 3136.68$ Å³, and $Z = 2$. The structure was refined with 6732 observed reflections having $F > 2.33\sigma(F)$, giving final R factors of 0.0602 and 0.0616 for R and R_w , respectively. Results of electronic, ¹H and ²H NMR, and EPR spectroscopy, fast atom bombardment mass spectrometry, and variable-temperature magnetic susceptibility studies of these materials and the use of Cr–oxo assemblies as isoelectronic models of the photosynthetic manganese assembly in high- S states are discussed.

Introduction

Cr has been determined to be required for normal carbohydrate and lipid metabolism.⁵ Cr deficiency in humans results in symptoms comparable with those associated with adult-onset diabetes and cardiovascular disease.⁶ Yet as much as 90% of the American population's daily intake is less than the recommended safe and adequate quantities of Cr.⁷ Despite its apparent importance, until most recently little was known about the structure and function of the biologically active form of Cr. The biologically active form of chromium appears to be LMWCr (low-molecular-weight chromium-binding substance), an anionic, carboxylate-rich oligopeptide possessing a molecular weight of ca. 1500 and four chromic ions (reviewed in ref 5b). LMWCr contains a multinuclear anion (probably oxide)-bridged Cr–carboxylate assembly⁸ and appears to potentially play a role in insulin activation by activating the insulin-dependent protein tyrosine kinase activity of insulin receptor,⁹ while also activating a membrane phosphotyrosine phosphatase.¹⁰ Both activation activities are dependent on the chromium content of LMWCr; chromium cannot be functionally replaced with any other transition metal ion commonly found in biological systems.^{9,10}

Yet the three-dimensional structure of the chromium assembly in LMWCr is unknown. Information on the structure of the assembly can come from the synthetic model approach.¹¹ For LMWCr, this would entail the synthesis and establishment of the exact structures and properties of chromium complexes capable of existence and their use as a well-characterized and sound starting point to suggest by extrapolation what may be occurring within LMWCr.

The four-electron oxidation of water to dioxygen is catalyzed by a tetranuclear oxide-bridged Mn assembly in the protein complex photosystem II.¹² This assembly, which is probably supported by protein-supplied carboxylate ligands,¹³ sequentially accumulates 4 oxidizing equiv, which current evidence suggests involves primarily Mn(III) → Mn(IV) oxidations.¹⁴ The oxidized forms of the enzyme are unstable and thus difficult to study; hence, little information is available on the structure of the assembly. Increasingly precise X-ray absorption studies have narrowed the range of possible three-dimensional arrangements of the four manganese ions in the assembly;^{14b} however, no synthetic tetranuclear manganese assembly prepared to date fits within the window of possible structures consistent with the X-ray studies. Indeed, efforts to prepare synthetic models have proved problematic.¹³ Fortunately Cr(III) is isoelectronic with Mn(IV), also favors octahedral coordination, and has a comparable ionic radius but is stable with regard to reduction. Thus, synthesis of stable Cr(III) systems structurally analogous to but more stable than oxidized forms of the enzyme could provide insight into the approximate three-dimensional structure of the tetramanganese site of the enzyme.

[⊗] Abstract published in *Advance ACS Abstracts*, September 15, 1997.

(1) University of Alabama.
 (2) Indiana University.
 (3) Washington University.
 (4) University of New Orleans.
 (5) (a) Mertz, W. *J. Nutr.* **1993**, *123*, 626. (b) Vincent, J. B. In *Encyclopedia of Inorganic Chemistry*; King, R. B., Ed.; John Wiley & Sons: Chichester, England, 1994; Vol. 2, pp 661–665.
 (6) Anderson, R. A. *Trace Elements in Human and Animal Nutrition*; Academic Press: Orlando, FL, 1987; Vol. 1, pp 225–244.
 (7) Anderson, R. A.; Kozlovsky, A. S. *Am. J. Clin. Nutr.* **1985**, *41*, 1177.
 (8) Davis, C. M.; Vincent, J. B. *Arch. Biochem. Biophys.* **1997**, *339*, 335.
 (9) Davis, C. M.; Vincent, J. B. *Biochemistry* **1997**, *36*, 4382.
 (10) Davis, C. M.; Sumrall, K. H.; Vincent, J. B. *Biochemistry* **1996**, *35*, 12963.

(11) Ibers, J. A.; Holm, R. H. *Science* **1980**, *209*, 223.
 (12) Christou, G.; Vincent, J. B. *Biochim. Biophys. Acta* **1987**, *895*, 259.
 (13) Vincent, J. B.; Christou, G. *ACS Symp. Ser.* **1988**, *372*, 238.
 (14) (a) Debus, R. J. *Biochim. Biophys. Acta* **1992**, *1102*, 269. (b) Yachandra, V. K.; Sauer, K.; Klein, M. P. *Chem. Rev.* **1996**, *96*, 2927.

Toward these objectives, herein are reported the synthesis and characterization of two new structural types of chromium–oxo–carboxylate complexes.

Experimental Section

Syntheses. All manipulations were performed under aerobic conditions, and all chemicals were used as received. $[\text{Cr}_3(\mu_3\text{-O})(\mu\text{-OAc})_6(\text{H}_2\text{O})_3]\text{Cl}$,¹⁵ $[\text{Cr}_3(\mu_3\text{-O})(\mu\text{-O}_2\text{CCD}_3)_6(\text{H}_2\text{O})_3]\text{Cl}$,¹⁶ and $[\text{Cr}_4(\mu_3\text{-O})_2(\mu\text{-OAc})_7(\text{bpy})_2]\text{PF}_6$ ¹⁷ were prepared as described in the literature or were available from previous work. The authenticity of these materials was checked by IR, electronic, and ¹H and ²H NMR spectroscopy and by fast atom bombardment (FAB) mass spectrometry. Elemental analyses were performed by Galbraith Laboratories, Knoxville, TN.

Caution! Appropriate care should be taken whenever perchlorate salts are manipulated.

$[\text{Cr}^{\text{III}}_2(\mu\text{-O})_2(\mu\text{-OAc})(\text{bpy})_2(\text{H}_2\text{O})_2]\text{ClO}_4 \cdot \text{bpy} \cdot [\text{bpyH}]\text{ClO}_4$ (1). A 7.39 g $[\text{Cr}_3(\mu_3\text{-O})(\mu\text{-OAc})_6(\text{H}_2\text{O})_3]\text{Cl}$ (12.0 mmol) was dissolved in molten (80 °C) bpy (20.6 g, 132 mmol), and the mixture was stirred at 80 °C for 4 h. The resulting pink-purple solution was combined with 1.2 L of H₂O (doubly deionized), and the mixture was stirred vigorously to precipitate excess bpy. After filtration, the purple-pink filtrate was stirred, and 3.00 g of KClO₄ (21.7 mmol) was added. After sitting 24 h, the resulting mixture was filtered to give a purple-pink solid (see below) and a red filtrate. Allowing the filtrate to sit for a minimum of 2 days, filtering, and washing the isolated solid with water gave red crystals of **1** in approximately 10% yield (based on Cr). Anal. Calcd (found) for C₄₂H₄₀N₈O₁₄Cl₂Cr₂: C, 47.78 (47.47); H, 3.81 (3.53); N, 10.61 (10.05); Cr, 9.85 (9.94). Selected IR data: 1620 (m), 1570 (m), 1320 (m), 1165 (m), 1090 (s, br), 770 (m), 755 (s), 730 (s), 720 (sh), 620 (s), 570 (m), 520 (m), 410 (m) cm⁻¹. $[\text{Cr}_2(\mu\text{-O})_2(\mu\text{-O}_2\text{CCD}_3)_2(\text{bpy})_2(\text{H}_2\text{O})_2]\text{ClO}_4 \cdot \text{bpy} \cdot [\text{bpyH}]\text{ClO}_4$ was prepared in an identical fashion starting with $[\text{Cr}_3(\mu_3\text{-O})(\mu\text{-O}_2\text{CCD}_3)_6(\text{H}_2\text{O})_3]\text{Cl}$.

$[\text{Cr}^{\text{III}}_3(\mu\text{-OH})_2(\mu\text{-OAc})_4(\text{OAc})_2(\text{bpy})_2]\text{ClO}_4 \cdot 1/6\text{CH}_2\text{Cl}_2 \cdot \text{H}_2\text{O}$. The isolated purple-pink solid from above was extracted with dichloromethane. The resulting pink solution was filtered, and the filtrate was layered with an equal volume of hexanes to give pink crystals of the dichloromethane solvate of **2**. The crystals rapidly lost solvent and crumbled when isolated. Samples for elemental analysis were dried under vacuum; the yield of dried material was ca. 40% (based on Cr). Anal. Calcd (found) for C_{32.17}H_{38.33}N₄O₁₉Cl_{1.33}Cr₃: C, 39.09 (39.02); H, 3.91 (3.67); N, 5.67 (5.35); Cr, 15.78 (16.22); Cl, 4.78 (4.19). Selected IR data: ~3500 (m, br), 1625 (s), 1600 (sh), 1100 (s), 1040 (m), 930 (m), 850 (w), 775 (s), 735 (s), 725 (sh), 675 (s), 655 (m), 620 (s), 570 (m), 460 (m), 425 (m) cm⁻¹. Samples for X-ray crystallography and magnetic susceptibility studies were recrystallized from CHCl₃/hexanes and removed directly from the mother liquor without drying under vacuum. These crystals also lost solvate with time. For elemental analysis, samples were dried under vacuum. Anal. Calcd (found) for $[\text{Cr}_3(\text{OH})_2(\text{OAc})_6(\text{bpy})_2]\text{ClO}_4 \cdot 2.5\text{CHCl}_3$ (C_{34.5}H_{38.5}N₄O₁₈Cl_{8.5}Cr₃): C, 33.03 (33.31); H, 3.09 (2.97); N, 4.47 (4.50); Cr, 12.43 (12.66). $[\text{Cr}_3(\mu\text{-OH})_2(\mu\text{-O}_2\text{CCD}_3)_4(\text{O}_2\text{CCD}_3)_2(\text{bpy})_2]\text{ClO}_4$ was prepared using an identical procedure starting with $[\text{Cr}_3(\mu_3\text{-O})(\mu\text{-O}_2\text{CCD}_3)_6(\text{H}_2\text{O})_3]\text{Cl}$.

X-ray Crystallography and Structure Solution. For compound **1**, a crystal of dimensions 0.45 × 0.27 × 0.17 mm was mounted on a glass fiber in random orientation. Preliminary examination and data collection were performed with a Siemens SMART charge coupled device (CCD) detector system single-crystal X-ray diffractometer using graphite monochromated Mo K α radiation equipped with a sealed tube X-ray source at 23 °C. Preliminary unit cell constants were determined with a set of 45 narrow-frame (0.3° in ω) scans. A total of 1300 frames of intensity data were collected with a frame width of 0.3° in ω and counting time of 10 s/frame at a crystal to detector distance of 3.9 cm. The double-pass method of scanning was used to exclude any noise. Data were collected at room temperature for a total time of 6.00 h. The collected frames were integrated using an orientation matrix determined from the narrow-frame scans. The SMART software

Table 1. Crystallographic Data for Complex **1**

chem formula: C ₄₂ H ₄₀ Cl ₂ Cr ₂ N ₈ O ₁₄	space group: <i>Cc</i>
fw = 1055.72	<i>T</i> = 296 K
<i>a</i> = 16.8259(8) Å	λ = 0.710 73 Å
<i>b</i> = 21.9622(11) Å	$\rho_{\text{cal}} = 1.535 \text{ g cm}^{-3}$
<i>c</i> = 14.6056(8) Å	$\mu = 6.68 \text{ cm}^{-1}$
$\beta = 122.1830(10)^\circ$	<i>R</i> = 0.0721 ^a
<i>V</i> = 4568.0(4) Å ³	<i>R</i> _w = 0.1305 ^b
<i>Z</i> = 4	

^a $R = \sum||F_o| - |F_c||/\sum|F_o|$. ^b $R_w = [\sum w(F_o^2 - F_c^2)^2/\sum w(F_o^2)^2]^{1/2}$, where $w = 1/[\sigma^2(F_o^2) + (0.0094P)^2 + 30.5189P]$ and $P = (F_o^2 + 2F_c^2)/3$.

Table 2. Selected Fractional Coordinates (×10⁴) and Isotropic Thermal Parameters (×10³) for Complex **1**

atom	<i>x</i>	<i>y</i>	<i>z</i>	<i>U</i> (eq), Å ²
Cr(1)	0	376(1)	0	38(1)
Cr(2)	1293(1)	66(1)	-705(2)	34(1)
O(1)	-44(4)	84(3)	-1328(6)	36(2)
O(2)	1234(4)	16(3)	586(6)	38(2)
O(3)	203(5)	602(3)	1374(6)	45(2)
O(4)	1161(5)	115(3)	-2127(6)	43(2)
O(5)	407(5)	1202(3)	-146(6)	48(2)
O(6)	1443(4)	960(3)	-589(6)	44(2)
C(21)	1027(7)	1347(4)	-352(9)	47(3)
C(22)	1256(9)	1996(4)	-325(13)	77(4)
N(1)	-1386(6)	640(4)	-781(8)	48(2)
N(2)	-653(7)	-421(4)	-70(8)	51(2)
N(3)	1414(6)	-862(3)	-696(7)	40(2)
N(4)	2752(6)	-23(4)	111(8)	46(2)
C(1)	-1667(7)	1227(6)	-994(9)	60(3)
C(2)	-2619(8)	1379(8)	-1486(11)	83(5)
C(3)	-3247(9)	946(9)	-1701(13)	96(5)
C(4)	-2948(8)	326(8)	-1456(11)	77(4)
C(5)	-2005(8)	194(6)	-1010(10)	59(3)
C(6)	-1595(8)	-413(5)	-673(10)	49(3)
C(7)	-2142(11)	-940(7)	-1011(13)	83(5)
C(8)	-1696(13)	-1465(7)	-654(15)	96(5)
C(9)	-733(12)	-1498(6)	32(14)	82(4)
C(10)	-234(9)	-945(6)	302(11)	62(3)
C(11)	702(9)	-1248(5)	-1104(11)	62(3)
C(12)	832(12)	-1869(6)	-980(14)	86(4)
C(13)	1713(15)	-2088(6)	-492(15)	100(6)
C(14)	2447(12)	-1709(7)	-122(14)	95(5)
C(15)	2294(9)	-1064(6)	-227(11)	63(3)
C(16)	3072(8)	-592(6)	197(10)	57(3)
C(17)	4020(9)	-718(8)	619(12)	86(5)
C(18)	4604(8)	-237(10)	937(12)	99(6)
C(19)	4321(9)	343(9)	907(12)	85(5)
C(20)	3357(7)	427(6)	438(10)	60(3)

package (Siemens Analytical X-ray, Madison, WI, 1994) was used for data collection, and Siemens SAINT software was used for frame integration. Analysis of the integrated data did not show any decay. Final cell constants were determined by a global refinement of *x*, *y*, *z* centroids of 4937 reflections. An empirical absorption correction was carried out using an ellipsoidal model (*T*_{max}/*T*_{min} = 0.902/0.853). The integration process yielded 15 089 reflections, of which 3653 ($2\theta < 50$) were independent. Data were reduced using SHELXTL-PLUS (PC version). The position of the two chromium atoms were determined using heavy-atom methods. Remaining non-hydrogen atoms were found by successive full-matrix refinements and difference Fourier map calculations. Final refinements were carried out using SHELXL-93, where full-matrix least-squares refinement was carried out by minimizing $\sum w(F_o^2 - F_c^2)^2$. The non-hydrogen atoms were refined anisotropically to convergence. The hydrogen atoms were refined using an appropriate riding model (AFIX m3). The associated perchlorate anions were found to be disordered, with three pairs of disordered oxygen atoms on Cl(1) (O(11)/O(11A), O(13)/O(13A) having 55/45% occupancies and O(14)/O(14A) having 70/30% occupancies) and one pair of disordered oxygen atoms on Cl(2) (O(21)/O(21A) with 55/45% occupancies). A summary of the experimental and structure solution procedure is given in Table 1. The final atomic coordinates are presented in Table 2.

(15) Johnson, M. K.; Powell, D. B.; Cannon, R. D. *Spectrochim. Acta* **1981**, *37A*, 995.

(16) Glass, M. M.; Belmore, K.; Vincent, J. B. *Polyhedron* **1993**, *12*, 133.

(17) Bino, A.; Chayat, R.; Pedersen, E.; Schneider, A. *Inorg. Chem.* **1991**, *30*, 856.

Table 3. Crystallographic Data for Complex **2**·5CHCl₃

chem formula: C ₃₇ H ₄₁ Cl ₁₆ Cr ₃ N ₄ O ₁₈	fw = 1552.98
<i>a</i> = 16.104(5) Å	space group: <i>P</i> $\bar{1}$
<i>b</i> = 17.623(5) Å	<i>T</i> = 98 K
<i>c</i> = 12.236(3) Å	λ = 0.710 69 Å
α = 93.33°	$\rho_{\text{cal}} = 1.644 \text{ g cm}^{-3}$
β = 92.81°	$\mu = 12.487 \text{ cm}^{-1}$
γ = 64.84(1)°	<i>R</i> = 0.0602 ^a
<i>V</i> = 3136.68 Å ³	<i>R</i> _w = 0.0616 ^b
<i>Z</i> = 2	

^a $R = \sum ||F_o| - |F_c|| / \sum |F_o|$. ^b $R_w = [\sum w||F_o| - |F_c||^2 / \sum w|F_o|^2]^{1/2}$, where $w = 1/\sigma^2(|F_o|)$.

For compound **2**, data were collected on a Picker four-circle diffractometer at -175 °C; details of the diffractometry, low-temperature facilities, and computational procedures employed by the Indiana MSC are available elsewhere.¹⁸ A systematic search of a limited region of reciprocal space revealed a set of diffraction maxima with no symmetry or symmetric absences, indicating a triclinic space group, later shown to be centrosymmetric *P* $\bar{1}$ by the subsequent solution and refinement of the structure. Following standard data reduction, correlation for Lorentz and polarization effects, and averaging of equivalent reflections, a unique set of 8184 reflections ($F > 2.33\sigma(F)$) was obtained. The structure was solved using a combination of direct methods (MULTAN78) and standard Fourier techniques. During the course of locating the atoms, it became apparent that several solvent molecules were present, with some disorder as well. Two CHCl₃ solvent molecules were well ordered (those with carbon atoms labeled 59 and 63), two were nearly disordered (carbon atoms labeled 67 and 71), and the solvent with carbons C(75) and C(75)' exhibited a nearly 50:50 disorder. After resolution of the disorder, a difference Fourier synthesis phased on the non-hydrogen atoms clearly located all hydrogen atoms (except those associated with disordered solvents), and these were refined isotropically in the final least-squares cycles. A final difference Fourier map was essentially featureless with the largest peaks (ca. 0.81 e/Å³) being in the vicinity of the solvents. Final *R* (*R*_w) values and a summary of the experimental and structure solution procedure are given in Table 3. The final atomic coordinates are presented in Table 4.

Physical Measurements. Infrared spectra (Nujol mull) were recorded on a Perkin-Elmer 283B spectrophotometer, and ¹H and ²H NMR spectra were obtained using a Bruker AM-360 and a Bruker AM-500 spectrometer, respectively, at ca. 23 °C. Chemical shifts are reported on the δ scale (shifts downfield are positive) using the solvent protio- and deuterio-component signal(s) as reference. A Hewlett-Packard 8451A spectrophotometer was used to record ultraviolet-visible spectra. FAB mass spectra were obtained using a VG Autospec high-resolution mass spectrometer, and EPR spectra were collected on a Varian E-12 spectrophotometer equipped with an Oxford ESR 900 cryostat.

The magnetic susceptibility data were recorded on 37.24 and 30.30 mg polycrystalline samples of compounds **1** and **2**, respectively, over the 2–300 K temperature range using a Quantum Design MPMS-5S SQUID susceptometer. Measurement and calibration techniques are

Table 4. Selected Fractional Coordinates ($\times 10^4$) and Isotropic Thermal Parameters ($\times 10$) for Complex **2**·5CHCl₃

atom	<i>x</i>	<i>y</i>	<i>z</i>	<i>B</i> _{iso} , Å ²
Cr(1)	431(1)	1823(1)	4056(1)	14
Cr(2)	-570(1)	3861(1)	3452(1)	15
Cr(3)	2526(1)	276(1)	3615(1)	14
N(4)	-1207(4)	4031(3)	1932(4)	20
C(5)	-998(6)	3444(4)	1115(6)	31
C(6)	-1441(7)	3595(5)	120(7)	43
C(7)	-2137(7)	4380(5)	-59(7)	44
C(8)	-2366(6)	4987(5)	772(6)	32
C(9)	-1893(5)	4795(4)	1774(6)	23
C(10)	-2088(5)	5400(4)	2727(6)	19
C(11)	-2760(5)	6212(4)	2727(6)	25
C(12)	-2888(5)	6715(4)	3666(7)	28
C(13)	-2333(5)	6400(4)	4567(6)	25
C(14)	-1669(5)	5598(4)	4525(6)	21
N(15)	-1538(4)	5097(3)	3618(4)	17
N(16)	3461(4)	-922(3)	3219(4)	16
C(17)	3488(5)	-1634(4)	3486(5)	19
C(18)	4087(5)	-2408(4)	3044(6)	22
C(19)	4661(5)	-2445(4)	2255(6)	25
C(20)	4650(5)	-1722(5)	1900(6)	25
C(21)	4045(4)	-959(4)	2355(5)	17
C(22)	3990(4)	-129(4)	2057(5)	16
C(23)	4611(5)	-32(5)	1410(6)	24
C(24)	4520(5)	782(5)	1259(6)	26
C(25)	3804(5)	1455(5)	1729(6)	23
C(26)	3208(5)	1306(4)	2363(6)	21
N(27)	3301(4)	539(3)	2543(4)	16
O(28)	233(3)	2716(3)	3103(4)	16
O(29)	1735(3)	1431(3)	3906(3)	16
O(30)	479(3)	2498(2)	5386(3)	16
C(31)	276(4)	3269(4)	5612(5)	16
O(32)	-98(3)	3855(3)	4966(4)	18
C(33)	526(5)	3472(4)	6755(6)	20
O(34)	-904(3)	2195(3)	4254(4)	18
C(35)	-1587(4)	2893(4)	4191(5)	16
O(36)	-1547(3)	3570(3)	3938(4)	18
C(37)	-2509(5)	2942(4)	4403(6)	22
O(38)	276(3)	4301(3)	2950(4)	20
C(39)	1105(5)	3923(4)	2655(6)	23
O(40)	1552(4)	3150(3)	2614(5)	39
C(41)	1553(6)	4469(5)	2337(8)	37
O(42)	329(3)	1126(3)	2774(3)	16
C(43)	896(4)	569(4)	2168(5)	17
O(44)	1750(3)	195(3)	2357(3)	16
C(45)	532(5)	311(5)	1118(6)	23
O(46)	599(3)	917(3)	5084(4)	17
C(47)	1226(4)	188(4)	5189(5)	16
O(48)	1925(3)	-151(2)	4621(3)	16
C(49)	1120(5)	-316(4)	6065(6)	22
O(50)	3414(3)	246(3)	4778(3)	18
C(51)	3424(5)	842(4)	5431(6)	21
O(52)	2873(4)	1579(3)	5388(5)	35
C(53)	4194(6)	565(5)	6275(6)	30
Cl(54)	4408(1)	3109(1)	644(1)	26
O(55)	5127(3)	2308(3)	857(4)	29
O(56)	4707(7)	3632(4)	165(7)	86
O(57)	3769(5)	2965(4)	-124(5)	66
O(58)	3932(4)	3488(3)	1617(4)	34

reported elsewhere.¹⁹ The temperature-dependent magnetic data were measured at a magnetic field of 1000 G.

Results and Discussion

Synthesis. Given the wide expanse of chemistry discovered for Mn-oxo-carboxylate-2,2'-bipyridine (bpy) systems,²⁰ an examination of similar systems for chromium(III) has been underway.²¹ Toward this end, the formation of these types of complexes using molten bpy as described by Bino and co-workers¹⁷ was reexamined. Previously it was reported that reaction of "mononuclear" chromic acetate, [Cr(H₂O)₆](OAc), or trinuclear [Cr₃(μ_3 -O)(μ -OAc)₆(H₂O)₃]Cl with molten bpy

(18) Chisholm, M. H.; Folting, K.; Huffman, J. C.; Kirkpatrick, C. C. *Inorg. Chem.* **1984**, *23*, 1021.

(19) O'Connor, C. J. *Prog. Inorg. Chem.* **1982**, *29*, 203.

(20) (a) Vincent, J. B.; Christmas, C.; Huffman, J. C.; Christou, G.; Chang, H.-R.; Hendrickson, D. N. *J. Chem. Soc., Chem. Commun.* **1987**, 236. (b) Christmas, C.; Vincent, J. B.; Huffman, J. C.; Christou, G.; Chang, H.-R.; Hendrickson, D. N. *J. Chem. Soc., Chem. Commun.* **1987**, 1303. (c) Vincent, J. B.; Christmas, C.; Chang, H. R.; Li, Q.; Boyd, P. D. W.; Huffman, J. C.; Hendrickson, D. N.; Christou, G. *J. Am. Chem. Soc.* **1989**, *111*, 2086. (d) Bashkin, J. S.; Schake, A. R.; Vincent, J. B.; Chang, H. R.; Li, Q.; Huffman, J. C.; Christou, G.; Hendrickson, D. N. *J. Chem. Soc., Chem. Commun.* **1988**, 700. (e) Menage, S.; Girerd, J. J.; Gleizes, A. *J. Chem. Soc., Chem. Commun.* **1988**, 431. (f) Menage, S.; Vitols, S. E.; Begerat, P.; Codjovi, E.; Kahn, O.; Girerd, J. J.; Guillot, M.; Solans, X.; Calvet, T. *Inorg. Chem.* **1991**, *30*, 2666. (g) Reddy, K. R.; Rajasekharan, M. V.; Padhye, S.; Dahan, F.; Tchuagues, J.-P. *Inorg. Chem.* **1994**, *33*, 428–433. (h) Dave, B. C.; Czernuszewicz, R. S.; Bond, M. R.; Carrano, C. J. *Inorg. Chem.* **1993**, *32*, 3593. (i) Vincent, J. B.; Folting, K.; Huffman, J. C.; Christou, G. *Biochem. Soc. Trans.* **1988**, *16*, 822.

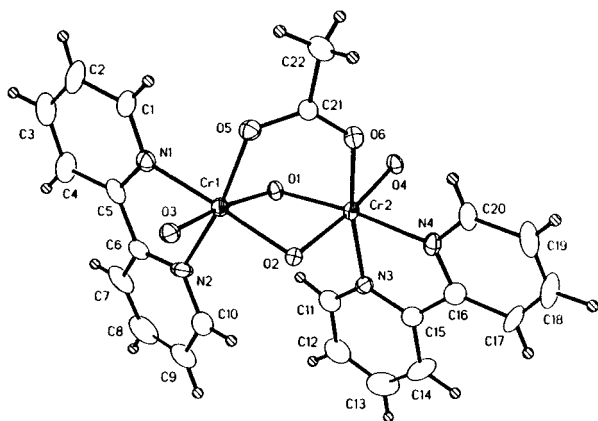
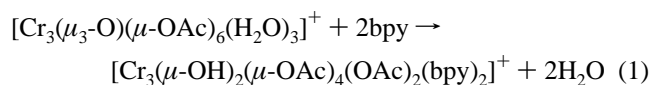


Figure 1. Structure of the cation of complex **1** showing the atom-labeling scheme.

followed by further processing gave the tetranuclear cation $[\text{Cr}_4(\mu_3\text{-O})_2(\mu\text{-OAc})_7(\text{bpy})_2]^+$ (**3**).¹⁷ However, the system appears to be quite complex and dependent on the nature of the starting Cr(III)-containing material.

Indeed, the use of the mononuclear starting material gives rise to the tetranuclear cation as reported previously; but in numerous attempts to use the trinuclear complex, the isolated product was not the tetranuclear cation. The material isolated after extraction of the bpy reaction mixture with water and addition of anion is the cation of compound **2**, $[\text{Cr}_3(\mu\text{-OH})_2(\mu\text{-OAc})_4(\text{OAc})_2(\text{bpy})_2]^+$. Use of KPF_6 (used by Bino *et al.*) instead of KClO_4 results in formation of the same cation as shown by IR, electronic, and ^1H NMR spectroscopy; thus the nature of the product is not dependent on the anion used. The IR and electronic spectra of the cation of **2** and the tetranuclear cation **3** are quite similar (*vide infra*); given the small scales of the reactions in ref 17, it is perhaps understandable how the differences in spectra depending on starting material could be overlooked. The nature of the starting materials used in this study were probed exhaustively²² to guarantee authentic material was being used.

The reaction giving rise to compound **2** is straightforward (eq 1). The aquo ligands of the starting trimer are somewhat



labile, being *trans* to the Cr(III)-oxo interaction;²³ this presumably allows replacement of the ligand by one pyridine ring of the bpy. Attack of the second N of the chelate would then trigger rearrangement of the cation. Yet the nature of this rearrangement is probably complex, given the formation of other products (such as compound **1** or what subsequently gives rise to **1**) in the reaction.

Description of the Structures. The structure of the cation of complex **1** is shown in Figure 1. Selected interatomic distances and angles are listed in Table 5. Complex **1** crystallizes in the space group *Cc*, such that the dinuclear cation contains no imposed symmetry. The cation is composed of a central dichromium(III) unit bridged by two oxo ligands and one acetato ligand. Octahedral coordination about each chromium is completed by a water molecule and a bidentate 2,2'-

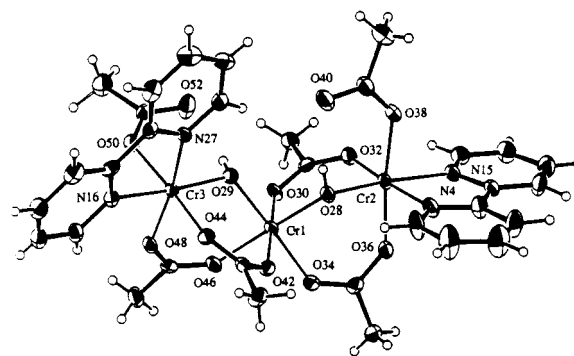


Figure 2. Structure of the cation of complex **2** showing the atom-labeling scheme. Carbon atoms are labeled consecutively from N and O atoms.

Table 5. Selected Interatomic Distances (Å) and Angles (deg) for Complex **1**

(a) Distances			
Cr(1)–O(3)	1.912(7)	Cr(1)–O(2)	1.944(6)
Cr(1)–O(5)	1.989(7)	Cr(1)–O(1)	2.007(7)
Cr(1)–N(2)	2.041(8)	Cr(1)–N(1)	2.060(8)
Cr(2)–O(2)	1.943(7)	Cr(2)–O(1)	1.925(6)
Cr(2)–O(6)	1.976(6)	Cr(2)–O(4)	1.972(7)
Cr(2)–N(4)	2.089(9)	Cr(2)–N(3)	2.048(7)
Cr(1)···Cr(2)	2.940(2)		
(b) Angles			
O(3)–Cr(1)–O(2)	95.2(3)	O(3)–Cr(1)–O(5)	89.9(3)
O(2)–Cr(1)–O(5)	94.0(3)	O(3)–Cr(1)–O(1)	172.3(3)
O(2)–Cr(1)–O(1)	77.1(3)	O(5)–Cr(1)–O(1)	91.4(3)
O(3)–Cr(1)–N(2)	93.7(3)	O(2)–Cr(1)–N(2)	95.3(3)
O(5)–Cr(1)–N(2)	169.6(3)	O(1)–Cr(1)–N(2)	86.3(3)
O(3)–Cr(1)–N(1)	91.4(3)	O(2)–Cr(1)–N(1)	170.9(3)
O(5)–Cr(1)–N(1)	92.1(3)	O(1)–Cr(1)–N(1)	96.2(3)
N(2)–Cr(1)–N(1)	78.1(4)	O(1)–Cr(2)–O(2)	79.1(3)
O(1)–Cr(2)–O(4)	93.0(3)	O(2)–Cr(2)–O(4)	172.1(3)
O(1)–Cr(2)–O(6)	94.8(3)	O(2)–Cr(2)–O(6)	92.5(3)
O(4)–Cr(2)–O(6)	88.4(3)	O(1)–Cr(2)–N(3)	96.4(3)
O(2)–Cr(2)–N(3)	89.7(3)	O(4)–Cr(2)–N(3)	90.9(3)
O(6)–Cr(2)–N(3)	168.8(3)	O(1)–Cr(2)–N(4)	173.2(4)
O(2)–Cr(2)–N(4)	95.3(3)	O(4)–Cr(2)–N(4)	92.5(3)
O(6)–Cr(2)–N(4)	89.2(3)	N(3)–Cr(2)–N(4)	79.7(3)

bipyridine. The bridging oxo groups have a *trans* influence resulting in the Cr–N distances *trans* to an oxide (2.060(8) Å, 2.089(9) Å) being longer than the distances from the chromium to the nitrogen of the other pyridine ring of the bipyridine ligands (2.041(8) Å, 2.048(7) Å). This arrangement results in idealized C_2 symmetry for the cation with the C_2 axis passing through the center of the $\text{Cr}_2(\mu\text{-O})_2$ rhomb.

Overall the structure of the cation is strikingly similar to that of its isoelectronic Mn(IV) analogue, $[\text{Mn}^{\text{IV}}_2(\mu\text{-O})_2(\mu\text{-OAc})(\text{bpy})_2(\text{H}_2\text{O})_2]^{3+}$,^{20g,h} which shares idealized C_2 symmetry (Table 7). The main differences between the structures of the Mn and Cr complexes stem in part from the higher charge and subsequent somewhat smaller ionic radii of the tetravalent Mn. Consequently, the longer Cr–oxo bonds contribute to the greater metal···metal separation, 2.940(2) Å, than in the Mn complex, 2.6401(5) Å.^{20g} The $\text{Cr}_2(\mu\text{-O})_2(\mu\text{-OAc})$ unit is found in the center of the tetranuclear cations $[\text{Cr}_4(\mu_3\text{-O})_2(\mu\text{-OAc})_7(\text{bpy})_2]^+$ ¹⁷ and $[\text{Cr}_4(\mu_3\text{-O})_2(\mu\text{-OAc})_7(\text{phen})_2]^+$.²¹ The Cr···Cr separations of the central $\text{Cr}_2(\mu\text{-O})_2$ rhomb of the tetranuclear cations are 2.7835(8) and 2.791(2) Å, respectively, with Cr–oxo distances averaging 1.903(3) and 1.895(7) Å, respectively. Given the nearly identical Cr–oxo distances in **1** and the tetranuclear species, other contributions must be responsible for the long Cr···Cr separation and large Cr–O–Cr angles in **1**.

Figure 2 displays the structure of the cation of complex **2**. Selected interatomic distances and angles are presented in Table 6. Complex **2**·5CHCl₃ crystallizes in the space group $P\bar{1}$, such

(21) Ellis, T.; Glass, M.; Harton, A.; Foltling, K.; Huffman, J. C.; Vincent, J. B. *Inorg. Chem.* **1994**, *33*, 5522.

(22) (a) Glass, M. M.; Belmore, K.; Vincent, J. B. *Polyhedron* **1993**, *12*, 133. (b) Belmore, K.; Madison, X. J.; Harton, A.; Vincent, J. B. *Spectrochim. Acta* **1994**, *50A*, 2365. (c) Vincent, J. B. *Inorg. Chem.* **1994**, *33*, 5604.

(23) Harton, A.; Nagi, M. K.; Glass, M. M.; Junk, P. C.; Atwood, J. L.; Vincent, J. B. *Inorg. Chim. Acta* **1994**, *217*, 171.

Table 6. Selected Interatomic Distances (Å) and Angles (deg) for Complex **2**·5CHCl₃

(a) Distances			
Cr(1)—O(28)	1.921(5)	Cr(1)—O(29)	1.926(5)
Cr(1)—O(30)	1.977(4)	Cr(1)—O(34)	1.987(4)
Cr(1)—O(42)	1.980(4)	Cr(1)—O(46)	2.009(4)
Cr(2)—O(28)	1.913(5)	Cr(2)—O(32)	1.967(4)
Cr(2)—O(36)	1.975(4)	Cr(2)—O(38)	1.969(5)
Cr(2)—N(4)	2.053(5)	Cr(2)—N(15)	2.076(5)
Cr(3)—O(29)	1.909(5)	Cr(3)—O(44)	1.973(4)
Cr(3)—O(48)	1.965(4)	Cr(3)—O(50)	1.953(4)
Cr(3)—N(16)	2.078(5)	Cr(3)—N(27)	2.052(5)
Cr(1)···Cr(2)	3.363(2)	Cr(1)···Cr(3)	3.360(2)
(b) Angles			
O(28)—Cr(1)—O(29)	89.34(20)	O(28)—Cr(1)—O(30)	92.97(18)
O(28)—Cr(1)—O(34)	92.79(19)	O(28)—Cr(1)—O(42)	89.52(18)
O(28)—Cr(1)—O(46)	177.90(19)	O(29)—Cr(1)—O(30)	90.16(19)
O(29)—Cr(1)—O(34)	177.85(19)	O(29)—Cr(1)—O(42)	92.59(18)
O(29)—Cr(1)—O(46)	92.38(19)	O(30)—Cr(1)—O(34)	89.48(18)
O(30)—Cr(1)—O(42)	176.31(18)	O(30)—Cr(1)—O(46)	85.82(17)
O(34)—Cr(1)—O(42)	87.68(17)	O(34)—Cr(1)—O(46)	85.49(18)
O(42)—Cr(1)—O(46)	91.61(18)	O(28)—Cr(2)—O(32)	95.00(18)
O(28)—Cr(2)—O(36)	93.06(21)	O(28)—Cr(2)—O(38)	94.08(20)
O(28)—Cr(2)—N(4)	93.01(20)	O(28)—Cr(2)—N(15)	171.77(20)
O(32)—Cr(2)—O(36)	91.03(19)	O(32)—Cr(2)—O(38)	90.74(19)
O(32)—Cr(2)—N(4)	171.88(20)	O(32)—Cr(2)—N(15)	93.11(20)
O(36)—Cr(2)—O(38)	172.47(19)	O(36)—Cr(2)—N(4)	87.25(20)
O(36)—Cr(2)—N(15)	85.38(19)	O(38)—Cr(2)—N(4)	89.98(21)
O(38)—Cr(2)—N(15)	87.22(20)	N(4)—Cr(2)—N(15)	78.86(21)
O(29)—Cr(3)—O(44)	92.10(19)	O(29)—Cr(3)—O(48)	95.02(19)
O(29)—Cr(3)—O(50)	94.06(19)	O(29)—Cr(3)—N(16)	172.03(22)
O(29)—Cr(3)—N(27)	93.56(21)	O(44)—Cr(3)—O(48)	92.53(18)
O(44)—Cr(3)—O(50)	173.23(18)	O(44)—Cr(3)—N(16)	86.50(19)
O(44)—Cr(3)—N(27)	88.35(19)	O(48)—Cr(3)—O(50)	89.73(19)
O(48)—Cr(3)—N(16)	92.88(19)	O(48)—Cr(3)—N(27)	171.34(19)
O(50)—Cr(3)—N(16)	87.01(19)	O(50)—Cr(3)—N(27)	88.47(20)
N(16)—Cr(3)—N(27)	78.57(21)	Cr(1)—O(28)—Cr(2)	122.64(26)
Cr(1)—O(29)—Cr(3)	122.35(24)		

that its trinuclear cation possesses no idealized or imposed symmetry. The cation consists of two (*μ*-hydroxo)bis(*μ*-acetato)dichromium(III) units which are “fused” at the central chromic center to give a [Cr(*μ*-OH)(*μ*-OAc)₂Cr(*μ*-OH)(*μ*-OAc)₂Cr]³⁺ core. Similar cores, [Mn^{III}(*μ*-OH)(*μ*-OAc)₂Mn^{II}(*μ*-OH)(*μ*-OAc)₂Mn^{III}]²⁺, [Fe^{III}(*μ*-OH)(*μ*-O₂CPh)₂Fe^{III}(*μ*-OH)(*μ*-O₂CPh)₂Fe^{III}]³⁺, and [Fe^{III}(*μ*-O)(*μ*-OAc)₂Fe^{III}(*μ*-OH)(*μ*-OAc)₂Fe^{III}]²⁺, have been observed in iron and manganese chemistry.^{24–26} This trinuclear core has not been known previously in chromium chemistry. However, unlike those in the Fe and Mn complexes, the bridging hydroxide ligands are arranged adjacent to each other about the central chromium rather than *trans*. The central chromium is in a pseudo-octahedral environment of oxygens provided by the six bridging ligands. Six-coordination about each terminal chromium is completed by a monodentate acetate ligand and a bidentate 2,2′-bipyridine ligand. The terminal carboxylates are H-bonded to the hydrogen of the bridging hydroxo groups (H(17)···O(40), 1.913 Å; H(18)···O(52), 1.986 Å). The short Cr···Cr separations are 3.363 Å (Cr(1)···Cr(2)) and 3.360 Å (Cr(1)···Cr(3)). The separations are very similar to the 3.381 Å separation found for the [Cr₂(*μ*-OH)(*μ*-O₂CH)₂]³⁺ core of [Cr₂(*μ*-OH)(*μ*-O₂CH)₂(H₂O)₆]³⁺.²⁷ While no single-atom bridge or simple ligand bridge connects terminal Cr(2)

and Cr(3) such that the trinuclear complex could be considered “linear”, the angle Cr(2)—Cr(1)—Cr(3) deviates appreciably from 180°, being 133.2°.

Magnetic Susceptibility Studies. The temperature-dependent magnetic susceptibility data for both compounds **1** and **2** exhibit Curie–Weiss paramagnetism at high temperatures. The magnetic data for the two compounds were fit to the Curie–Weiss law (eq 2). The data for [Cr₂(*μ*-O)₂(*μ*-OAc)(bpy)₂(H₂O)₂]-

$$\chi = C/(T - \Theta) = Ng^2\mu_B^2 S(S + 1)/[3k(T - \Theta)] \quad (2)$$

ClO₄·bpy·[bpyH]ClO₄ are plotted as inverse magnetic susceptibility in Figure 3. The resulting least-squares-fitted parameters are $C = 3.98 \text{ emu} \cdot \text{K} \cdot \text{mol}^{-1}$ and $\Theta = 3.13 \text{ K}$. The small value for Θ suggests that the two chromic centers are weakly antiferromagnetically coupled. The magnetic exchange expected for a binuclear chromium(III) system can be described using a Heisenberg isotropic Hamiltonian model, $H = -2JS_1S_2$. The best least-squares fit of the data over the entire temperature range to the $S = 3/2$ binuclear model gave the following parameters: $g = 2.20$, $J/k = -0.40 \text{ K}$, and $\text{TIP} = 0.0049 \text{ emu/mol}$. The small value of the coupling constant is consistent with the Curie–Weiss behavior of the compound. This in stark contrast to the coupling between the isoelectronic Mn(IV) centers of its isostructural Mn^{IV} analogue ($J/k = -47$,^{20h} -30 ,^{320g} K) (literature J values were converted from cm^{-1} to K using the relationship $hck^{-1} = 1.44 \text{ K/cm}^{-1}$). The difference may reflect the larger metal–oxide bond distances (and resulting longer metal···metal separations and larger metal–oxide–metal angles) of the chromic complex, even though the orbital overlap in the central rhombs of both isostructural species should be reasonably similar (*vide infra*). However, a larger number of isostructural Cr(III) and Mn(IV) multinuclear complexes need to be available for similar comparisons.

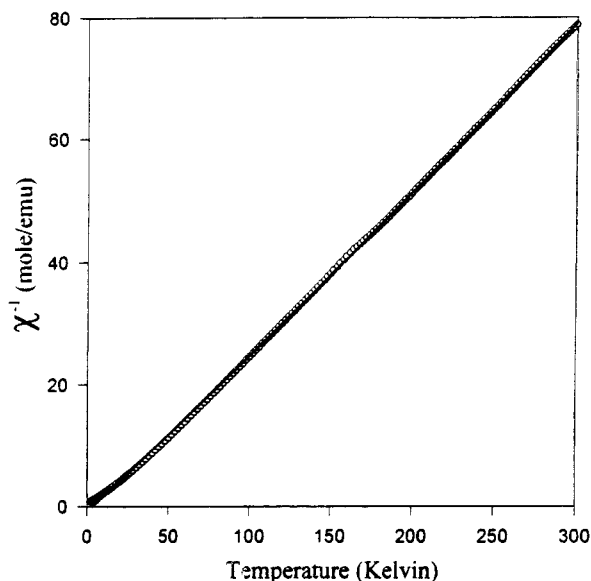
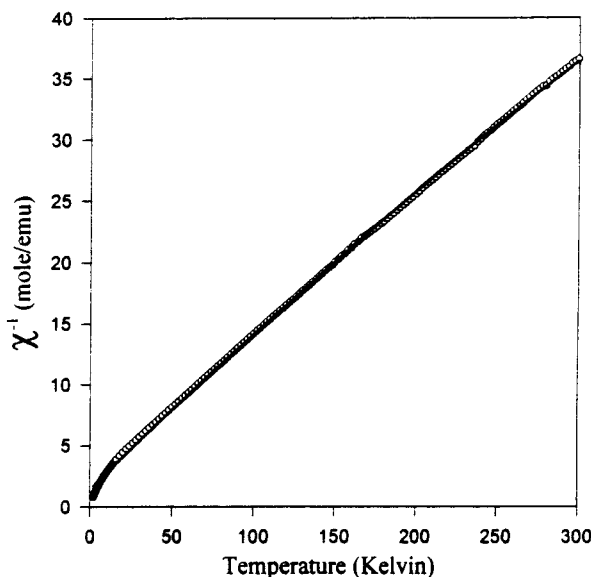
The data for [Cr₃(*μ*-OH)₂(*μ*-OAc)₄(OAc)₂(bpy)₂]ClO₄·5CHCl₃ are plotted in Figure 4 as inverse magnetic susceptibility. The resulting least-squares-fitted parameters are $C = 7.45 \text{ emu} \cdot \text{K} \cdot \text{mol}^{-1}$ and $\Theta = -10.91 \text{ K}$. The small value of Θ is consistent with a weak antiferromagnetic coupling between the chromium centers. The magnetic susceptibility of the trinuclear chromium(III) complex was fit over the entire temperature range to a theoretical model using the trimeric spin Hamiltonian $H = -2J(S_1S_2 + S_2S_3 + S_3S_1)$. The parameters from the best least-squares fit to the $S = 3/2$ system are as follows: $g = 2.18$, $J/k = -0.571 \text{ K}$, and $\text{TIP} = 0.00023 \text{ emu/mol}$. As in the case of the dimer, the small value of the coupling constant is consistent with the Curie–Weiss behavior of the compound. (Satisfactory fits were obtained without the inclusion of terms of intermolecular interactions.)

Spectroscopy and Spectrometry. Paramagnetic ¹H and ²H NMR spectroscopy has been demonstrated to be of utility in characterizing antiferromagnetically-coupled chromium(III) assemblies.^{16,21–23} For chromic ions, d³, each of the three unpaired electrons occupies a t_{2g} orbital (assuming typical octahedral coordination), directed between the chromium–ligand bonds. Hence, a π -delocalization mechanism is expected to be the major contributor to the paramagnetic shifts, especially as d³ octahedral complexes are magnetically isotropic such that dipolar shifts should be quite small or negligible. The ¹H NMR spectrum of **2** displays resonances over the range ca. +45 to –90 ppm (Figure 5 and Table 8). Resonances from acetate methyl protons (+44.3, +42.8, +16.6, +15.7 ppm) were readily assigned by comparing the spectrum of the deuterated analogue, [Cr₂(*μ*-OH)₂(*μ*-O₂CCD₃)₄(O₂CCD₃)₂(bpy)₂]ClO₄; resonances from 2,2′-bipyridine protons were assigned by comparison of the spectrum with those of similar Cr(III)–bpy complexes.²¹ The acetate resonances at +44.3 and +42.8 ppm correspond to the

- (24) Kitajima, N.; Amagai, H.; Tamura, N.; Ito, M.; Moro-oka, Y.; Heerwegh, K.; Penicaud, A.; Mathur, R.; Reed, C. A.; Boyd, P. D. W. *Inorg. Chem.* **1993**, *32*, 3583.
- (25) Vankai, V. A.; Newton, M. G.; Kurtz, D. M., Jr. *Inorg. Chem.* **1992**, *31*, 341.
- (26) Kitajima, N.; Tamura, N.; Amagai, H.; Fukui, H.; Moro-oka, Y.; Mizutani, Y.; Kitagawa, T.; Mathur, R.; Heerwegh, K.; Reed, C. A.; Randall, C. R.; Que, L., Jr.; Tatsumi, K. *J. Am. Chem. Soc.* **1994**, *116*, 9071.
- (27) Turowski, P. N.; Bino, A.; Lippard, S. J. *Angew. Chem., Int. Ed. Engl.* **1990**, *29*, 811

Table 7. Comparison of Selected Bond Distances and Angles for Complex **1** and Isostructural Mn Complexes

compd	M- μ -O, Å	M \cdots M, Å	M-O-M, deg	ref
1	1.955(7)	2.940(2)	97.5(3)	this work
[Mn ₂ (μ -O) ₂ (μ -OAc)(bpy) ₂ (H ₂ O) ₂] ³⁺	1.797(1)	2.6401(5)	94.51(5)	20g
[Mn ₂ (μ -O) ₂ (μ -OAc)(bpy) ₂ (H ₂ O) ₂] ³⁺	1.794(4)	2.642	94.8(2)	20h

**Figure 3.** Inverse magnetic susceptibility of complex **1** plotted as a function of temperature over the 1.7–300 K temperature region. The line drawn through the data is the fit to the Curie-Weiss model as described in the text.**Figure 4.** Inverse magnetic susceptibility of complex **2** plotted as a function of temperature over the 1.7–300 K temperature region. The line drawn through the data is the fit to the Curie-Weiss model as described in the text.

bridging carboxylates, as the greater shifts result from interactions with two chromic centers. The resonances at +16.6 and +15.7 ppm are shifted somewhat less than expected for monodentate acetate bound to a chromic center;⁸ however, this is readily explained by the antiferromagnetic coupling between the metal centers of **2**, which lowers the effective magnetic moment of the chromic ions. Additionally, the signals at +44.3 and +42.8 ppm integrate to approximately twice the area of the signals at +16.6 and +15.7 ppm. The lack of symmetry of **2** is disclosed by the number of observed acetate resonances (also the bpy protons at +24.6 ppm appear to be a doublet). This is more clearly shown in the ²H NMR spectrum of the

deuterio analogue of **2** (Figure 6); five resonances are now observable at +43.6, +42.3, +41.7, +16.4, and +15.4 ppm in a ratio of 2:1:1:1:1. The increased resolution of the bridging acetate signals results from the ²H NMR line widths, which can be up to 42 times smaller than those of the corresponding ¹H line widths ($\gamma_{\text{H}}^2/\gamma_{\text{D}}^2 = 42.4$, $\gamma =$ gyromagnetic ratio).²⁸ Unfortunately, all attempts to obtain two-dimensional NMR spectra of this complex were unsuccessful as a result of the short relaxation times.²⁹

The ¹H NMR spectrum of complex **1** proved to be quite complex. The only common NMR solvent in which **1** was found to dissolve was acidic D₂O (2% DCl). In addition to resonances expected from free [bpyH]⁺ and the solvent protio component, six resonances were observed over the range +60 to -60 ppm: +36.9, +22.3, +1.92, +1.13, -30.9, and -33.2 ppm. The signals at +36.9 and +1.92 ppm disappear in the spectrum of [Cr₂(μ -O)₂(μ -O₂CCD₃)(bpy)₂(H₂O)₂]ClO₄·bpy·[bpyH]ClO₄ and thus may be assigned to acetate methyl protons, with the signal at +1.92 corresponding to free acetic acid. The presence of free acetic acid represents decomposition of complex **1**. Surprisingly, ²H NMR spectra of the deuterioacetate analogue of **1** in 2% HCl revealed four signals from O₂CCD₃ in addition to the uncoordinated acid at ~+52, +39.4, +35.3, and +30.7 ppm; obviously, complex **1** decomposes upon dissolution, resulting in the production of numerous products, which can be resolved by ²H NMR as a result of the decreased line widths. The relative ratio of the four signals does not vary significantly over the HCl range of 0.5–10%; however, the ratio of these four signals to that of free acetic acid decreased rapidly with increasing acidity.

FAB mass spectrometry was also recently shown to be a valuable technique for the characterization of cationic multinuclear Cr assemblies.^{22b,c,23} FAB mass spectra of compound **2** reveal that the parent cation, [Cr₃(μ -OH)₂(μ -OAc)₄(OAc)₂(bpy)₂]⁺ (mass 856), represents the most intense feature. Fragments deriving from the trinuclear cation are also observed: [Cr₃O₂(OAc)₄(bpy)₂]⁺ (736, 11% intensity relative to the parent cation), resulting from the loss of 2 HOAc; [Cr₃O(OH)(OAc)₅(bpy)₂]⁺ (640, 66%), resulting from loss of [bpyH]-OAc; and [Cr₃O(OH)(OAc)₄(bpy)₂]⁺ (581, 23%). As compound **1** decomposes or fails to dissolve in all solvents examined to date, no matrix suitable for FAB could be identified.

The X-band EPR spectrum of a CH₂Cl₂/toluene solution of complex **2** at 10.7 K (Figure 7) reveals prominent features at $g = 5.11$, 4.12, and 2.01 but also numerous additional weaker features. Thus, it is apparent that, even at 10.7 K, numerous spin states are occupied and contributing to the spectrum. This would appear to be consistent with the small value of J determined from the variable-temperature susceptibility data.

The electronic spectrum of complex **2** is shown in Figure 8 and is somewhat similar in profile to that of tetranuclear [Cr₄(μ_3 -O)₂(μ -OAc)₇(bpy)₂]⁺.¹⁷ Yet the former compound is distinctly pink while the latter is purple; this is manifested by the differing energies of their absorption features. The electronic spectrum of **2** is dominated by a broad band with a maximum at 538 nm ($\epsilon/\text{Cr} = 65.5$) while the spectrum of the tetranuclear species possesses a similar band with a maximum at 562 nm ($\epsilon/\text{Cr} = 55$).

(28) Johnson, A.; Everett, G. W. *J. Am. Chem. Soc.* **1972**, *94*, 1419.(29) Wang, Z.; Holman, T. R.; Que, L., Jr. *J. Magn. Reson.* **1993**, *578*.

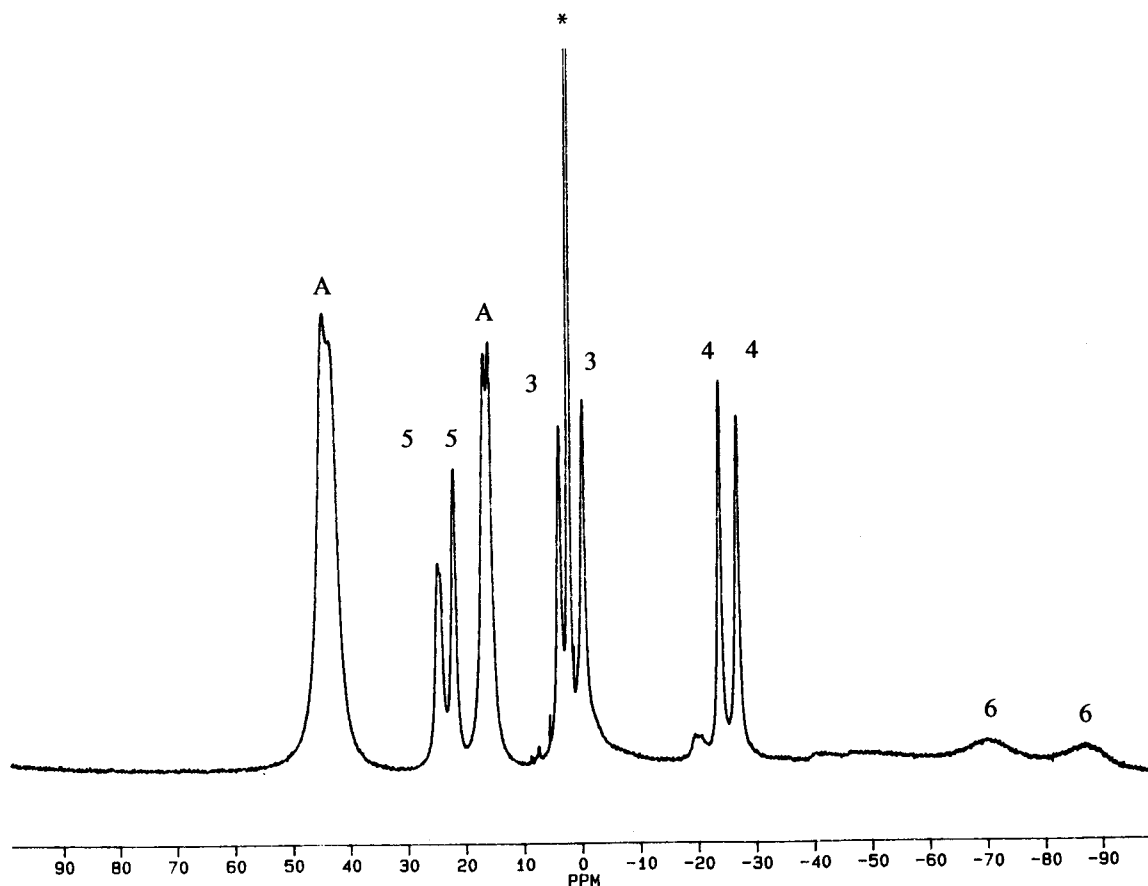


Figure 5. ^1H NMR spectrum of complex **2** in CD_3CN . Key: *, solvent proton component; A, acetate; numbers correspond to the positions of protons of 2,2'-bipyridine.

Table 8. ^1H NMR Resonances of Compound **2** and Assignments and Relaxation Rates

assignt	δ , ppm	T_1 , ms	assignt	δ , ppm	T_1 , ms
OAc ^a	+44.3	0.56	3	+3.7	1.6
OAc ^a	+42.8	0.56	3	-0.42	1.6
5 ^b	+24.6	1.4	4	-23.9	3.0
5	+24.1	1.4	4	-27.0	2.8
OAc ^c	+16.6	1.0	6	~-71	<i>d</i>
OAc ^c	+15.7	1.0	6	~-88	<i>d</i>

^a Bridging. ^b Numbers correspond to bpy ring positions. ^c Terminal. ^d Resonances too broad to accurately determine T_1 's.

The spectrum of **2** also possesses another feature at higher energy with a maximum at 390 nm ($\epsilon/\text{Cr} = 94.8$) and a shoulder at 410 nm. The feature maximal at 538 nm is readily assigned on the basis of its intensity to a d-d transition of the chromic ions. Another d-d transition may underlie the higher energy feature. The structure on the higher energy feature resembles shoulders seen between ca. 350 and 400 nm in other oxo-bridged chromium carboxylate assemblies which have been assigned to simultaneous pair excitation (SPE) transitions.³⁰

Discussion and Conclusions

The number of types of multinuclear anion-bridged chromium(III) carboxylate assemblies is rapidly expanding and now includes members possessing Cr_2O ,³¹ Cr_2OH ,^{27,32} Cr_2O_2 , sym-

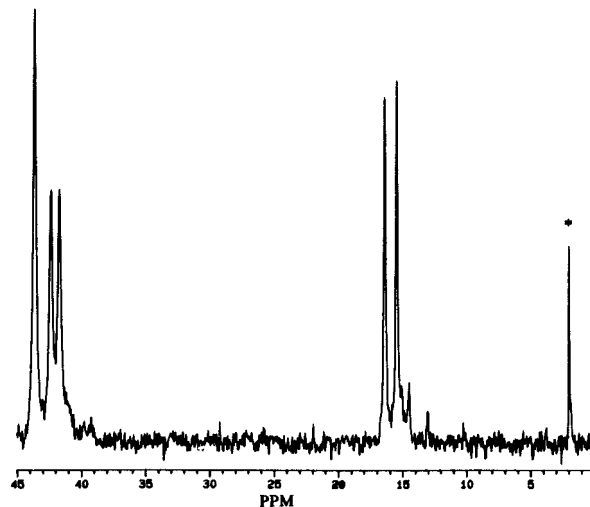


Figure 6. ^2H NMR spectrum of $[\text{Cr}_3(\mu\text{-OH})_2(\mu\text{-O}_2\text{CCD}_3)_4(\text{O}_2\text{-CCD}_3)_2(\text{bpy})_2]\text{ClO}_4$ in CH_3CN . Key: *, solvent deutero component.

metric¹⁴ and unsymmetric³³ Cr_3O , linear $\text{Cr}_3(\text{OH})_2$, Cr_4S ,³⁴ Cr_4O_2 ,^{17,21} Cr_8F_8 ,³⁵ and $\text{Cr}_{12}\text{O}_{12}$ ³⁶ cores. Most of the lower nuclearity (2-4) assemblies have isostructural Mn(III) and Fe(III) analogues; however, prior to this work, no isoelectronic and isostructural chromium and manganese or iron analogues had been reported. Chromium(III) complexes could serve as

(30) Dublicki, L.; Day, P. *Inorg. Chem.* **1972**, *11*, 1868.

(31) (a) Gafford, B. G.; Marsh, R. E.; Schaefer, W. P.; Zhang, J. H.; O'Connor, C. J.; Holwerda, R. A. *Inorg. Chem.* **1990**, *29*, 4652-4657. (b) Martin, L. L.; Wieghardt, K.; Blondin, G.; Girerd, J.-J.; Nuber, B.; Weiss, J. J. *Chem. Soc., Chem. Commun.* **1990**, 1767.

(32) (a) Brudenell, S. J.; Crimp, S. J.; Higgs, J. K. E.; Moubarak, B.; Murray, K. S.; Spiccia, L. *Inorg. Chim. Acta* **1996**, *247*, 35. (b) Green, C. A.; Koine, N.; Legg, J. I.; Willet, R. D. *Inorg. Chim. Acta* **1990**, *176*, 87.

(33) Nagi, M. K.; Harton, A.; Donald, S.; Lee, Y.-S.; Sabat, M.; O'Connor, C. J.; Vincent, J. B. *Inorg. Chem.* **1995**, *34*, 3813.

(34) Bino, A.; Johnston, D. C.; Goshorn, D. P.; Halbert, T. R.; Stiefel, E. I. *Science* **1988**, *241*, 1479.

(35) Gerbeleu, N. V.; Struchkov, Yu. T.; Timko, G. A.; Batsanov, A. S.; Indrichan, K. M.; Popovich, G. A. *Dokl. Akad. Nauk SSSR* **1990**, *313*, 1459.

(36) Batsanov, A. S.; Timko, G. A.; Struchkov, Yu. T.; Gerbeleu, N. V.; Indrichan, K. M. *Koord. Khim.* **1991**, *17*, 662.

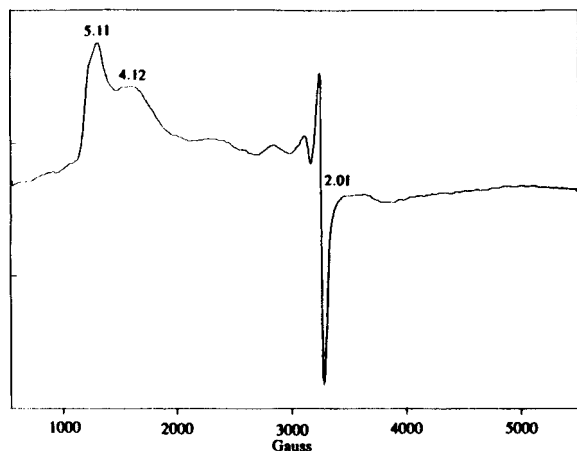


Figure 7. X-band EPR spectrum of complex **2** as a saturated 1:1 $\text{CH}_2\text{-Cl}_2$ /toluene solution at 10.7 K. Conditions: gain, 6.3×10^4 ; scan time, 2 min; time constant, 0.5 s; modulation amplitude, 10 G; field set, 3000 G; scan range, 5000 G; power, 0.2 mW; frequency, 9.05 GHz.

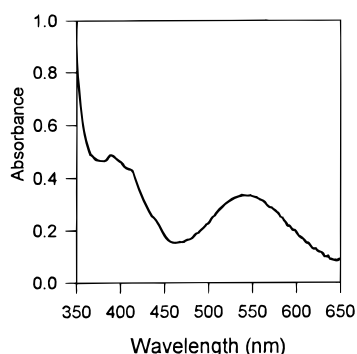


Figure 8. Electronic spectrum of complex **2** in CHCl_3 . $[\text{Cr}] = 5.15 \times 10^{-3}$ M.

stable isostructural and isoelectronic analogues of the higher S states of the tetranuclear photosynthetic manganese assembly, which is composed primarily, if not in some oxidation level solely, of Mn(IV). For example, both Mn(IV) and Cr(III) prefer octahedral coordination. Cr(III) may also stabilize peroxide ligands,^{37,38} a probable intermediate in photosynthetic water oxidation.³⁹ The dinuclear complex reported in this work establishes the plausibility of synthesizing isoelectronic and isostructural analogues of Mn(IV) species. A similar approach to generating isostructural (but not isoelectronic) photosynthetic manganese assembly mimics was reported recently using Co(III).⁴⁰

This laboratory has shown that reactions of "basic carboxylate"-type trinuclear chromic assemblies serve as convenient routes to the synthesis of new Cr(III)-oxo(hydroxo)-carboxylate species. This chemistry utilizing the trinuclear starting materials has resulted in the preparation of dinuclear, linear trinuclear, unsymmetric trinuclear,³³ and tetranuclear²¹ assemblies. The trimers are readily prepared (often in one-pot syntheses),²³ are soluble in numerous organic solvents allowing for reaction conditions to be widely varied, and are sources of carboxylate, oxide, and Cr(III). The availability of new chromium-oxo(hydroxo)-carboxylate species is important to provide a database of spectroscopic properties of such assemblies for comparison against the properties of LMWCr to aid in the elucidation of the latter's structure. For example,

(37) (a) Ardon, M.; Bleicher, B. *J. Am. Chem. Soc.* **1966**, *88*, 858. (b) Adams, A. C.; Crook, J. R.; Bockhoff, F.; King, E. L. *J. Am. Chem. Soc.* **1968**, *90*, 5761.

(38) Dickman, M. H.; Pope, M. T. *Chem. Rev.* **1994**, *94*, 569.

(39) Krishtalik, L. I. *Biochim. Biophys. Acta* **1986**, *849*, 162.

(40) Dimitrou, K.; Folting, K.; Streib, W. E.; Christou, G. *J. Am. Chem. Soc.* **1993**, *115*, 6432.

LMWCr possesses a broad ^1H NMR resonance at ca. +40 ppm, which was assigned to methylene protons of the carboxylate groups of aspartate or glutamate residues bridging two chromic centers which were additionally bridged by an oxo ligand.⁸ This study shows that the proton resonance could result from protons on methylene carbons of similar carboxylate groups bridging two chromic centers additionally bridged by a hydroxo rather than an oxo ligand, as the acetate methyl proton resonances of complex **2** fall in this area (ca. +40 ppm).

Unfortunately, the insolubility and instability (in those solvents in which it dissolved) of complex **1** prevent a detailed comparison of its spectroscopic properties with those of its Mn^{IV}_2 analogue. However, the magnetic properties of complex **1** and its isoelectronic and isostructural manganese analogue are very distinct, despite reasonably similar overlaps of orbitals. The differences between complex **1** and its manganese analogue warrant further discussion. The Cr...Cr separation in **1** is 0.300 Å shorter than the metal separation in the dimanganese complex. The radii for six-coordinate Cr^{3+} and Mn^{4+} are approximately 0.755 and 0.670 Å,⁴¹ respectively, a difference of only 0.085 Å. Therefore, the difference in metal...metal separations as a result of the difference in ionic radii is expected to be at most 0.170 Å, significantly less than the observed difference. As described earlier, the long Cr...Cr distance may arise as the result of the long Cr-O(oxide) distances, averaging 1.967 Å. In contrast, the bonds average 1.79 Å in the Mn analogue (Table 7). Thus, the difference between the average metal-oxide distances in the two cations (~ 0.18 Å) is much greater than expected from the difference in ionic radii. Another difference between the Mn and Cr complexes is in the significance of the *trans* influence exerted by the bridging oxides. For the Mn complex, the Mn-N bonds *trans* to the oxide are on average 0.042 Å longer than the other Mn-N bonds.^{20g,h} This difference is only 0.030 Å in complex **1**. Taken together, these results suggest that the Mn-O(oxide) bonds possess significantly more π (double-bond) character than the Cr-O(oxide) bonds, resulting in the greater *trans* influence and shorter bond lengths in the former. This is consistent with the results of the magnetic susceptibility studies. The increase in π character of the Mn-O(oxide) bonds would thus allow for greater coupling of the unpaired electrons on the metal centers via superexchange through these μ_2 -oxides. This is consistent with recent density functional calculations indicating a strong metal-ligand covalency of oxo ligands with Mn(IV) sites of dinuclear Mn assemblies which cannot be explained by the position of the ligand in the spectrochemical series.⁴²

Thus, while chromium complexes may not reproduce in detail the bond distances etc. of their isostructural and isoelectronic manganese analogues, this study shows that such chromium and manganese analogues can be prepared and that tetranuclear chromium complexes could potentially be prepared. Efforts to synthesize and characterize additional isostructural and isoelectronic chromium analogues of known Mn(IV) assemblies are currently underway.

Acknowledgment is made to the donors of the Petroleum Research Fund, administered by the American Chemical Society (J.B.V.), and to the American Heart Association (J.B.V.) for support of this research.

Supporting Information Available: Tables of crystallographic data, fractional coordinates, thermal parameters, and bond distances and angles for **1** and **2** and a labeling scheme for the anion and [bipyH]- ClO_4 of **1** (27 pages). Ordering information is given on any current masthead page.

IC961247T

(41) Shannon, R. D. *Acta Crystallogr.* **1976**, *A32*, 751.

(42) Zhao, X. G.; Richardson, W. H.; Chen, J.-L.; Li, J.; Noodleman, L.; Tsai, H.-L.; Hendrickson, D. N. *Inorg. Chem.* **1997**, *36*, 1198.